Experimental verification of negative refraction for a wedge-type negative index metamaterial operating at terahertz

Shengxiang Wang, Frédéric Garet, Karine Blary, Eric Lheurette, Jean-Louis Coutaz, Didier Lippens

▶ **To cite this version:**

Shengxiang Wang, Frédéric Garet, Karine Blary, Eric Lheurette, Jean-Louis Coutaz, et al.. Experimental verification of negative refraction for a wedge-type negative index metamaterial operating at terahertz. Applied Physics Letters, 2010, 97, pp.181902. 10.1063/1.3511540 . hal-00991478

HAL Id: hal-00991478
https://hal.science/hal-00991478v1

Submitted on 27 May 2022

HAL is a multi-disciplinary open access archive for the deposit and dissemination of scientific research documents, whether they are published or not. The documents may come from teaching and research institutions in France or abroad, or from public or private research centers.

L'archive ouverte pluridisciplinaire **HAL**, est destinée au dépôt et à la diffusion de documents scientifiques de niveau recherche, publiés ou non, émanant des établissements d'enseignement et de recherche français ou étrangers, des laboratoires publics ou privés.

Applied Physics Letters

Experimental verification of negative refraction for a wedge-type negative index metamaterial operating at terahertz

Cite as: Appl. Phys. Lett. **97**, 181902 (2010); https://doi.org/10.1063/1.3511540
Submitted: 27 July 2010 • Accepted: 15 October 2010 • Published Online: 01 November 2010

Shengxiang Wang, Frédéric Garet, Karine Blary, et al.

View Online Export Citation

ARTICLES YOU MAY BE INTERESTED IN

Experimental verification of backward-wave radiation from a negative refractive index metamaterial
Journal of Applied Physics **92**, 5930 (2002); https://doi.org/10.1063/1.1513194

Origin of dissipative losses in negative index of refraction materials
Applied Physics Letters **82**, 2356 (2003); https://doi.org/10.1063/1.1563726

Microwave transmission through a two-dimensional, isotropic, left-handed metamaterial
Applied Physics Letters **78**, 489 (2001); https://doi.org/10.1063/1.1343489

Lock-in Amplifiers up to 600 MHz
Zurich Instruments
Watch

AIP Publishing

© 2010 American Institute of Physics.

Experimental verification of negative refraction for a wedge-type negative index metamaterial operating at terahertz

Shengxiang Wang,[1] Frédéric Garet,[2] Karine Blary,[1] Eric Lheurette,[1] Jean Louis Coutaz,[2] and Didier Lippens[1,a)]

[1]*Institut d'Électronique de Microélectronique et Nanotechnologies, UMR 8520, Université des Sciences et Technologies de Lille, Avenue Poincaré BP 60069, 59652 Villeneuve d'Ascq Cedex, France*

[2]*Laboratoire IMEP-LAHC, UMR CNRS 5130, Université de Savoie, Site de Chambery Bâtiment Chablais, 73376 Le Bourget du Lac Cedex France*

(Received 27 July 2010; accepted 15 October 2010; published online 1 November 2010)

We report on angle-resolved time domain spectroscopy (TDS) carried out on a prismlike negative index metamaterial operating around 0.5 THz. The wedge-type devices are constituted of hole arrays etched in gold thin films, which are stacked according to a sequential mask shift. By means of a goniometric TDS setup and subsequent analysis of the temporal waveforms, negative refraction is demonstrated with values close to n=−1 around 0.5 THz. The dispersion of refractive index retrieved from the Snell–Descartes law shows comparable trends in comparison with the dispersion deduced from complex transmission and reflection measurements on slab-type samples. © *2010 American Institute of Physics*. [doi:10.1063/1.3511540]

Electromagnetic metamaterial technologies are now attracting much interest owing to their singular effective parameters (effective permittivity and permeability) which allow notably the fabrication of single and double negative media.[1] On this basis, an unprecedented control of the electromagnetic wave propagation can be foreseen by using, in particular, optical transformation techniques.[2] First principle proofs but also practical applications which include the demonstration of negative refraction,[3] focusing with a flat lens,[4] and cloaking,[5] were reported in the last decade with preliminary demonstrations often at microwaves. The extension of these studies at higher frequencies and notably in the Terahertz (THz) spectral range is still challenging. The first and perhaps the most important difficulty stems from the requirement of a resonant current loop, as in the generic so-called split ring resonator technology,[6] which induces an artificial magnetic moment under grazing incidence. This key issue explains why most of the present works in the THz frequency range have addressed preferably metasurfaces[7,8] based on resonant electrical dipoles rather than bulk metamaterials. Clearly the scaling of the underlying concept for artificial magnetism to THz frequencies requires developing other excitation techniques under front side illumination. The so-called subwavelength hole array[9–11] technology and fishnet technologies[12–14] are two suitable routes toward this goal with so far the demonstrations of left-handedness at millimeter/submillimeter wavelengths and in the infrared spectral region. At THz frequencies, very interesting results were published with S-type interconnected patterns under grazing and normal incidence.[15] In the far infrared spectral region, we have shown that backward propagation of electromagnetic waves can be achieved with a stack of hole arrays with elliptical apertures.[16] The experimental verification in this case was carried out by means of the measurement of the reflection and transmission characteristics, in magnitude and phase, and subsequent retrieval of the dispersion of the effective permittivity and permeability via a Fresnel inversion technique. The operating mode which explains how a negative index material can be achieved in such hole array devices are discussed in the Refs. 9 and 17–21 on the basis of full wave electromagnetic simulations and lumped element circuit approach.

In the present paper, we target a *direct* experimental verification of the achievement of negative refractive index at THz frequency by the characterization of hole-array wedge-type devices. Therefore, contrary to the aforementioned assessment by using slabs,[16] through vector network analysis and retrieval techniques, we measure here the transmitted magnitude and the direction of propagation of the electromagnetic fields refracted by a prismlike device. We then deduce the effective index via the Snell–Descartes law.

Figure 1(a) gives a schematic of the basic cell which consists in an elliptical hole aperture etched in a thin metal foil. It can be shown numerically and assessed experimentally that the highest transmissivity is achieved for an optimal elliptical aspect ratio (EAR=d_y/d_x=1.8, where d_y and d_x are the small and large axis of the ellipse) and the polariza-

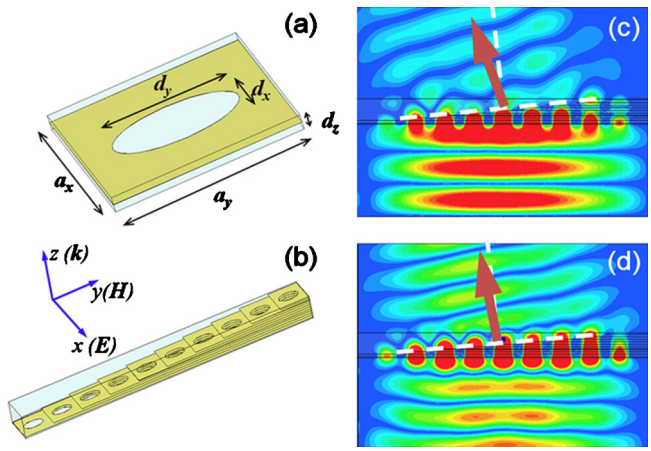

FIG. 1. (Color online) Schematic of the wedge-type devices: (a) one unit cell and (b) ten layers prism. Simulation of electric field mapping for a ten-stair prism at (a) 0.46 THz and (d) 0.49 THz.

a)Electronic mail: didier.lippens@iemn.univ-lille1.fr.

 © 2010 American Institute of Physics

tion conditions depicted in the Fig. 1(a) inset for which the electric field direction is along the small axis d_x. As shown recently,[22] the necessary condition to induce backward wave propagation is to stack at least two elementary hole array of this type which are coupled in our case by a dielectric spacer layer.

Further details about the underlying propagation mechanisms which combine the propagation of surface plasmonlike wave along the metal plate and a dissymmetrical coupling (odd eigenstates) via the dielectric spacer layer can be found in Ref. 23. Owing to the stack configuration of the sample under test, the electromagnetic properties are highly anisotropic. As a consequence, according to the trihedron $\boldsymbol{E}$, $\boldsymbol{H}$, $\boldsymbol{k}$ displayed in Fig. 1, where $\boldsymbol{E}$, $\boldsymbol{H}$, and $\boldsymbol{k}$ are, respectively, the electric field, magnetic field, and wave vectors, only the terms ε_{zz} and μ_{zz} of the effective permittivity and permeability tensors exhibit negative values. Under this condition, the more direct means to demonstrate negative refraction is to use a prismlike device with an incident wave impinging on the flat side of the triangular shaped cross section and the observation of the negative refraction at the tilted interface. Let us mention that negative refractive index was also demonstrated, under tilted incidence, for a slab of stacked subwavelength hole arrays.[24] Figure 1(b) gives a schematic of such a wedge-type device with a stairlike titled interface due to structuring. Again, it is worth mentioning that the orientation of the hole aperture has to satisfy the above criterion for high transmissivity, namely, with a polarization of $\boldsymbol{E}$ along $\boldsymbol{x}$. The frequency for which backward propagation, and thus subsequent negative refraction, is observed can be adjusted via the geometrical parameters and notably the periodicities of the basic cell via a_x and a_y, which determine the eigenstates of the surface waves and of the hole aperture which satisfies sub wavelength criterion. For a targeted operating frequency around 0.5 THz, the geometrical parameters are the following: $a_y=a_x=340$ μm, $d_x=125$ μm, and $d_y=225$ μm. With a thickness of the dielectric layer $d_z=26$ μm, a value of the wedge angle can be estimated to 4.4°.

With these parameters and for a prototype which consists in ten stacked metal layers, Figs. 1(c) and 1(d) illustrate the propagation of the electromagnetic wave through the mapping of the magnitude of the electric field component. The $\boldsymbol{E}$ field maps are here plotted for two representative frequencies for which negative refraction is expected on the basis of the dispersion characteristic of the corresponding slab. Figure 1(c) corresponds to an operating frequency f_{op} equal to 0.46 THz which roughly matches the threshold frequency where a left-handed dispersion branch is observed for a slab-type device. For such an operating condition, a large negative value of the refractive index, (in practice close to $n_{\text{eff}}=-3$ see Fig. 2) is expected along with a low transmissivity due to a poor impedance matching. From Fig. 1(c) It can be seen that the refracted beam is in the same half space than the incident one, assessing negative refraction. Figure 1(d) was computed for $f_{op}=0.49$ THz. Negative refraction is also verified in this case with, however, a refracted beam direction closer to the normal to the tilted interface and improved transmission showing a decrease in the negative value of the refractive index and a transmissivity increase.

The technological procedures, used for the fabrication of the devices, are comparable to those implemented for the fabrication of membranelike slab devices.[11] In short, the metal surfaces were achieved by sputtering 400 nm thick Au thin films. The patterning of holes was achieved by photolithography with a Microposit S1828 positive resist (Shipley Co.) and subsequent chemical Au etching. The dielectric spacer layers are fabricated from the benzocyclobutene resist, supplied by the Dow Chemical Co.. They were deposited by spin coating and subsequent annealing under a nitrogen controlled atmosphere at a temperature around 300 °C. The process is repeated according to a sequential mask shift in order to fabricate the stairlike microstructure displayed in Fig. 1(b). At last, the membrane was realized by means of a deep backside wet chemical etching ($H_2SO_4:H_2O_2:H_2O=1:8:1$). Photos of the completed sample along with a zoom view of the prism are shown in Figs. 3(a) and 3(b).

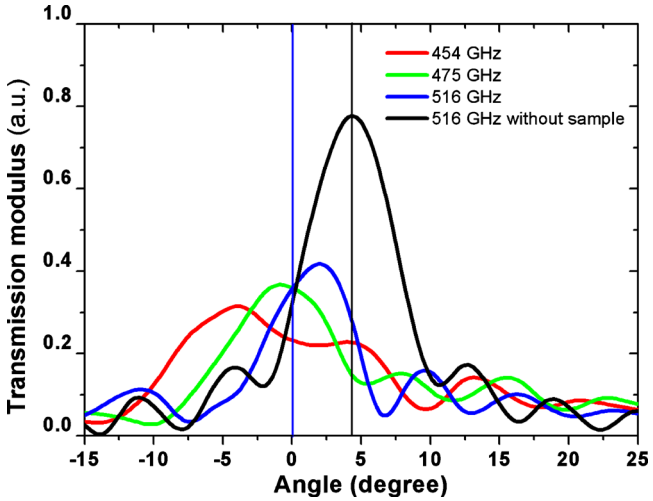

FIG. 2. (Color online) Transmission modulus as a function of the refracted beam angle for a prism with ten stacked hole arrays.

Figure 4 is a schematic of the goniometric setup. The angle-resolved transmission measurements were performed with a homemade TDS set up[25] using a Ti:sapphire laser excitation (50 fs pulse duration for a repetition rate of 100 MHz) and conventional dipole antennas, printed onto low temperature grown GaAs substrates. The collimation of the linearly polarized THz beam was achieved by means of high resistivity silicon hyper hemispherical lenses with a typical diameter of 15 mm attached to the antennas. The detector is placed at D=15 cm from the sample and hence in the far field ($D/\lambda \sim 250$ at 0.5 THz). It is rotating around the central axis of the sample holder as illustrated by the dashed lines. An optical fiber with a compensation of the group velocity dispersion gives enough flexibility to the set up so that the transient response of the refracted THz beam can be recorded for various angles.

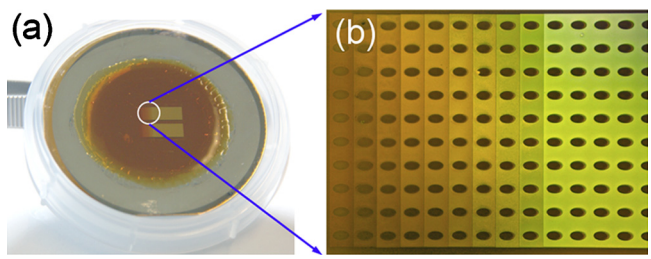

FIG. 3. (Color online) Photograph of the prism structure device (a) and of an optical microscope zoomed view of the prism with ten stacked hole arrays (b).

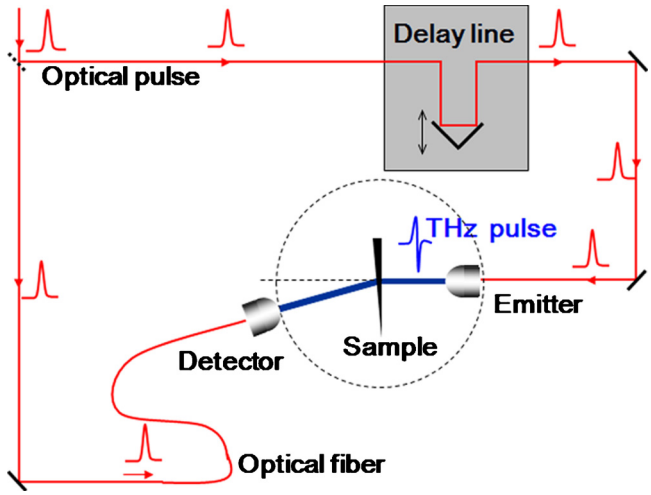

FIG. 4. (Color online) Schematic of the goniometric setup with the illustration of the optical and THz pulses in red and blue, respectively, and of the Si lenses in detection and emission (unscaled in this schematic).

In Fig. 2, we report the magnitude of the transmitted beam versus the angular position (θ) of the detector. The reference θ=0 corresponds to the normal to the tilted interface. The other angle reference corresponds to a straight through transmission without sample used in practice for the experiments (θ=4.4°). These angle-resolved data in the frequency domain have been derived after the Fourier transform of the transient response in the time domain measured experimentally. It can be seen that the refracted beam shifts progressively from the negative value for θ to the positive one by increasing the operating frequency. The difference in the level of transmission can be explained by the various impedance matching conditions as discussed in the previous sections.

Figure 5 compares the dispersion characteristics deduced from the Snell–Descartes (experiment) and from the numerical simulation of a five-layer slab (Fresnel inversion) and of a ten-layer wedge-type device (far field). For the three plots,

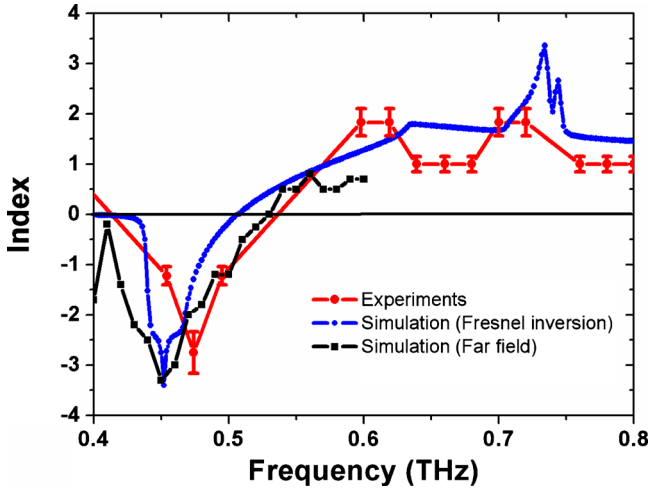

FIG. 5. (Color online) Frequency dependence of the effective refractive index deduced from experiment and compared to the variations calculated for slab- and prism-devices.

similar trends can be noticed with a strong dispersion of the refractive index (from n_{eff}=−3 up to n_{eff} close to 1) over a bandwidth around 0.1 THz corresponding to a fractional bandwidth (FBW) around 20%. As expected, FBW is broader for a prismlike configuration due to an expected spatial dispersion. A slight frequency shift can also be noted between calculation and experiment attributed to the tolerances in the devices fabrication.

In conclusion, a direct experimental evidence of negative refraction was achieved via angle-resolved measurements of a THz pulse refracted by a stack of metal hole array. A strong dispersion was pointed out experimentally in agreement with full wave analysis and subsequent retrieval of the frequency dependence of the effective refractive index. It is believed that such a high dispersive metamaterial could find useful applications in THz biosensors or chemical-sensors based on a refracted angle detection scheme.

[1]F. Capolino, *Metamaterials Handbook* (CRC, Great Britain, 2009).
[2]M. Rahm, D. A. Roberts, J. B. Pendry, and D. R. Smith, Opt. Express **16**, 11555 (2008).
[3]F. Zhang, G. Houzet, E. Lheurette, D. Lippens, M. Chaubet, and X. Zhao, J. Appl. Phys. **103**, 084312 (2008).
[4]K. Aydin, I. Bulu, and E. Ozbay, Opt. Express **13**, 8753 (2005).
[5]D. Schurig, J. J. Mock, B. J. Justice, S. A. Cummer, J. B. Pendry, A. F. Starr, and D. R. Smith, Science **314**, 977 (2006).
[6]J. B. Pendry, A. J. Holden, D. J. Robbins, and W. J. Stewart, IEEE Trans. Microwave Theory Tech. **47**, 2075 (1999).
[7]T. J. Yen, W. J. Padilla, N. Fang, D. C. Vier, D. R. Smith, J. B. Pendry, D. N. Basov, and X. Zhang, Science **303**, 1494 (2004).
[8]H.-T. Chen, W. J. Padilla, M. J. Cich, A. K. Azad, R. D. Averitt, and A. J. Taylor, Nat. Photonics **3**, 148 (2009).
[9]M. Beruete, M. Sorolla, and I. Campillo, Opt. Express **14**, 5445 (2006).
[10]M. Navarro-Cía, M. Beruete, M. Sorolla, and I. Campillo, Opt. Express **16**, 560 (2008).
[11]C. Croënne, F. Garet, E. Lheurette, J.-L. Coutaz, and D. Lippens, Appl. Phys. Lett. **94**, 133112 (2009).
[12]S. Zhang, W. Fan, N. C. Panoiu, K. J. Malloy, R. M. Osgood, and S. R. J. Brueck, Phys. Rev. Lett. **95**, 137404 (2005).
[13]G. Dolling, C. Enkrich, M. Wegener, C. M. Soukoulis, and S. Linden, Opt. Lett. **31**, 1800 (2006).
[14]J. Valentine, S. Zhang, T. Zentgraf, E. Ulin-Avila, D. A. Genov, G. Bartal, and X. Zhang, Nature (London) **455**, 376 (2008).
[15]H. O. Moser, J. A. Kong, L. K. Jian, H. S. Chen, G. Liu, M. Bahou, S. M. P. Kalaiselvi, S. M. Maniam, X. X. Cheng, B. I. Wu, P. D. Gu, A. Chen, S. P. Heussler, S. bin Mahmood, and L. Wen, Opt. Express **16**, 13773 (2008).
[16]S. Wang, F. Garet, K. Blary, C. Croënne, E. Lheurette, J. L. Coutaz, and D. Lippens, J. Appl. Phys. **107**, 074510 (2010).
[17]M. Beruete, I. Campillo, M. Navarro-Cía, F. Falcone, and M. Sorolla Ayza, IEEE Trans. Antennas Propag. **55**, 1514 (2007).
[18]M. Beruete, M. Navarro-Cía, I. Campillo, F. Falcone, I. Arnedo, and M. Sorolla, Opt. Quantum Electron. **39**, 285 (2007).
[19]R. Marquès, F. Mesa, L. Jelinek, and F. Medina, Opt. Express **17**, 5571 (2009).
[20]R. Marquès, L. Jelinek, F. Mesa, and F. Medina, Opt. Express **17**, 11582 (2009).
[21]J. Carbonell, C. Croënne, F. Garet, E. Lheurette, J. L. Coutaz, and D. Lippens, J. Appl. Phys. **108**, 014907 (2010).
[22]M. Beruete, M. Sorolla, M. Navarro-Cía, F. Falcone, I. Campillo, and V. Lomakin, Opt. Express **15**, 1107 (2007).
[23]A. Mary, S. G. Rodrigo, F. J. Garcia-Vidal, and L. Martin-Moreno, Phys. Rev. Lett. **101**, 103902 (2008).
[24]M. Beruete, M. Navarro-Cía, M. Sorolla, and I. Campillo, Phys. Rev. B **79**, 195107 (2009).
[25]Y. Laamiri, F. Garet, and J.-L. Coutaz, Appl. Phys. Lett. **94**, 071106 (2009).